

# The energy distance for ensemble and scenario reduction

Florian Ziel

October 11, 2021

## Abstract

Scenario reduction techniques are widely applied for solving sophisticated dynamic and stochastic programs, especially in energy and power systems, but also used in probabilistic forecasting, clustering and estimating generative adversarial networks (GANs). We propose a new method for ensemble and scenario reduction based on the energy distance which is a special case of the maximum mean discrepancy (MMD). We discuss the choice of energy distance in detail, especially in comparison to the popular Wasserstein distance which is dominating the scenario reduction literature. The energy distance is a metric between probability measures that allows for powerful tests for equality of arbitrary multivariate distributions or independence. Thanks to the latter, it is a suitable candidate for ensemble and scenario reduction problems. The theoretical properties and considered examples indicate clearly that the reduced scenario sets tend to exhibit better statistical properties for the energy distance than a corresponding reduction with respect to the Wasserstein distance. We show applications to a Bernoulli random walk and two real data based examples for electricity demand profiles and day-ahead electricity prices.

**Keywords:** energy score, Wasserstein metric, Kantorovic distance, scenario reduction, stochastic programming, maximum mean discrepancy, electricity load

## 1 Introduction and Motivation

In the operations research and optimization literature, ensemble and scenario reduction plays an important role for solving dynamic and stochastic programs. There are algorithms to find an (approximately) optimal solution by valuating simulated trajectories/paths from uncertain processes which are involved in the optimization problem. However, subsequent optimization steps are usually very costly in terms of computational effort - therefore ensemble or scenario reduction is applied. This holds especially with regard to applications for power and energy systems, see e.g. Growe-Kuska et al. (2003); Di Somma et al. (2018); Biswas et al. (2019); Gzafroudi et al. (2019). Further, reduction techniques reduce the computational effort and memory requirements in all applications where ensembles and scenarios are relevant. This is for instance in reporting probabilistic forecasts Gneiting and Katzfuss (2014), estimating generative adversarial networks (esp. Wasserstein-GANs and MMD-GANs) Li et al. (2017); Genevay et al. (2017), clustering Rizzo and Székely (2016), and visualization Wang et al. (2018).

Based on a (weighted) set of simulated trajectories or paths, a reduction technique is applied. The target for *ensemble reduction* is to find an *optimal* subset of  $m$  paths out of the simulated ensemble set with  $n$  paths, where  $m < n$ , see Fig. 1a and 1b for illustration. Thus, the weight distribution of the scenarios remain unchanged. In the equally weighted case (Fig. 1a) all trajectories in the reduced ensemble receive a weight of  $1/m$ , in Fig. 1b, the remaining weights are scaled to sum up to 1. Alongside with the classification also used in Rujeerapaiboon et al. (2018), in (discrete) *scenario reduction* (compare Fig. 1c) we aim to find not only the  $m$  subset paths but also the *optimal* associated probabilities. Thus, scenario reduction is usually a more sophisticated problem than ensemble reduction. Even more advanced and related to clustering methods is *continuous scenario reduction* (also known as scenario generation, see Fig. 1d). There we are looking for  $m$  new paths and weights that approximate the target distribution well. Which method is required depends a lot on the underlying problem. In this manuscript, we do not focus on continuous scenario reduction. Whenever we talk about scenario reduction, we mean discrete scenario reduction.

Obviously, the crucial question is: What means *optimal* in our context? In the ensemble and scenario reduction literature, different criteria for optimality are suggested. An important selection criterion is the choice of a distance (or metric) which characterizes to a certain extent how close the  $m$  selected trajectories are to the considered large set of  $n$  trajectories in the scenario set. The vast majority of articles favor the Wasserstein type distances resp. metrics (also Fortet-Mourier distance Kantorovich/Kantorovich-Rubinstein distance, earth mover distance, optimal transport distance) for scenario reduction, see Rujeerapaiboon et al. (2018); Glanzer and Pflug (2020). This also holds for all applications mentioned in the first paragraph. There are two main reasons: On the one hand, there are useful stability results in stochastic programming for the Wasserstein metric available. They guarantee under mild assumptions on the stochastic programme that a scenario reduction that approximates the full scenario set well leads to close to optimal solutions of the stochastic optimization problem, see e.g. Römisch (2003);

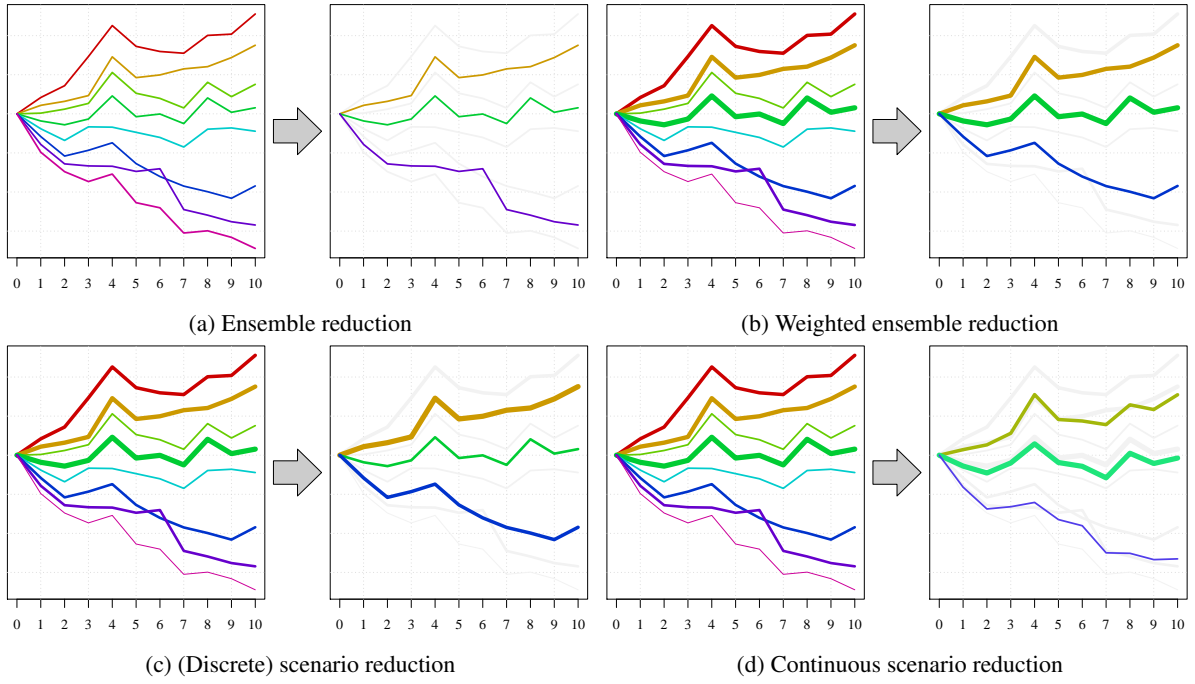


Figure 1: Illustration of ensemble and scenario reduction principles.

Rujeerapaiboon et al. (2018) for more details. On the other hand there is the fast scenario reduction method proposed by Dupačová et al. (2003), along with the implementation in the General Algebraic Modeling System (GAMS) by the software *Scenred*. It is based on the Wasserstein distance and the optimal redistribution rule (see e.g. Growe-Kuska et al. (2003)). It represents the reduction problem as a (mass) transportation problem which has an explicit solution for the scenario reduction problem. As the Wasserstein distance is a metric for probability measure that characterizes weak convergence of measures, it seems to be a suitable candidate for reduction problems. For instance Rujeerapaiboon et al. (2018) states: ‘*The modern stability theory of stochastic programming indicates that the distance may serve as a natural candidate for this probability metric.*’ in favor for the Wasserstein distance for scenario reduction problems. However, there are reduction techniques based on other distances, such as the discrepancy distances Henrion et al. (2009) and methods which are not based on probability distances, e.g. reduction techniques based on Euclidean distances, sampling or clustering Keko and Miranda (2015); Park et al. (2019); Zhou et al. (2019).

In this article, we present an alternative to the Wasserstein type distances based reduction techniques. We propose the energy distance (also known as energy statistic) for ensemble and scenario reduction, see Székely and Rizzo (2013). The energy distance is a special case of the maximum mean discrepancy (MMD) which is popular in machine learning, see Borgwardt et al. (2006). In applications, it often shows preferable statistical/stochastic properties for reduction problems in contrast to Wasserstein distance based approaches. To motivate this more appropriately, we show a small example, illustrated in Figure 2.

Fig 2a shows the considered set of 4 scenarios  $\mathbf{y}_1, \dots, \mathbf{y}_4$  with  $\mathbf{y}_i = (y_{i,1}, \dots, y_{i,9})$  on which we want to apply a scenario reduction so that the final set contains only 2 weighted trajectories. Figure 2d illustrates the main characteristics of the original ensemble, the first two moments with respect to the time dimension: Formally, the mean  $\boldsymbol{\mu} = \mathbb{E}\mathbf{Z}$  and standard deviation  $\boldsymbol{\sigma} = \sqrt{\text{diag}(\text{Cov} \mathbf{Z})}$  of the 9-dimensional uniform random variable  $\mathbf{Z}$  on the four atoms  $\mathbf{y}_1, \dots, \mathbf{y}_4$ , thus  $\mathbf{Z} \sim \mathcal{U}(\{\mathbf{y}_1, \mathbf{y}_2, \mathbf{y}_3, \mathbf{y}_4\})$ . Figures 2b and 2c show the trajectories of the best scenario reduction for the energy distance and Wasserstein distance with corresponding weights<sup>1</sup>. As in 2d, Figures 2e and 2f provide the mean and standard deviation of the reduction results with some approximation characteristics.

To understand the reduction results, we study the considered scenario set. It contains 4 scenarios, the first three of them tend to increase over time, the remaining trajectory 4 (purple) tends to decrease. Both scenario reduction techniques eliminate two of the increasing trajectories in the optimal solution. The Wasserstein reduction is based on the optimal redistribution rule (see Dupačová et al. (2003)). In consequence, the weights of the eliminated trajectories are redistributed to the remaining paths. In Figure 2c, the weights of trajectories 2 (green) and 3 (cyan) are redistributed to trajectory 1 (red) with a final weight of 75%, while keeping the remaining 25% for trajectory 4. On the first view this makes sense, as the trajectory 1 (red) tends to be the most centered one out of the three increasing trajectories. Indeed, if we would consider a classical transportation problem, this is the best choice. However, in many applications we use the remaining trajectories for sophisticated path-dependent optimization problems. Hence, we should care about the statistical/stochastic properties of the reduced scenario

<sup>1</sup>The reduction is computed with respect to  $d_{E,1}$  in (10) and  $d_{W,1}$  in (6)

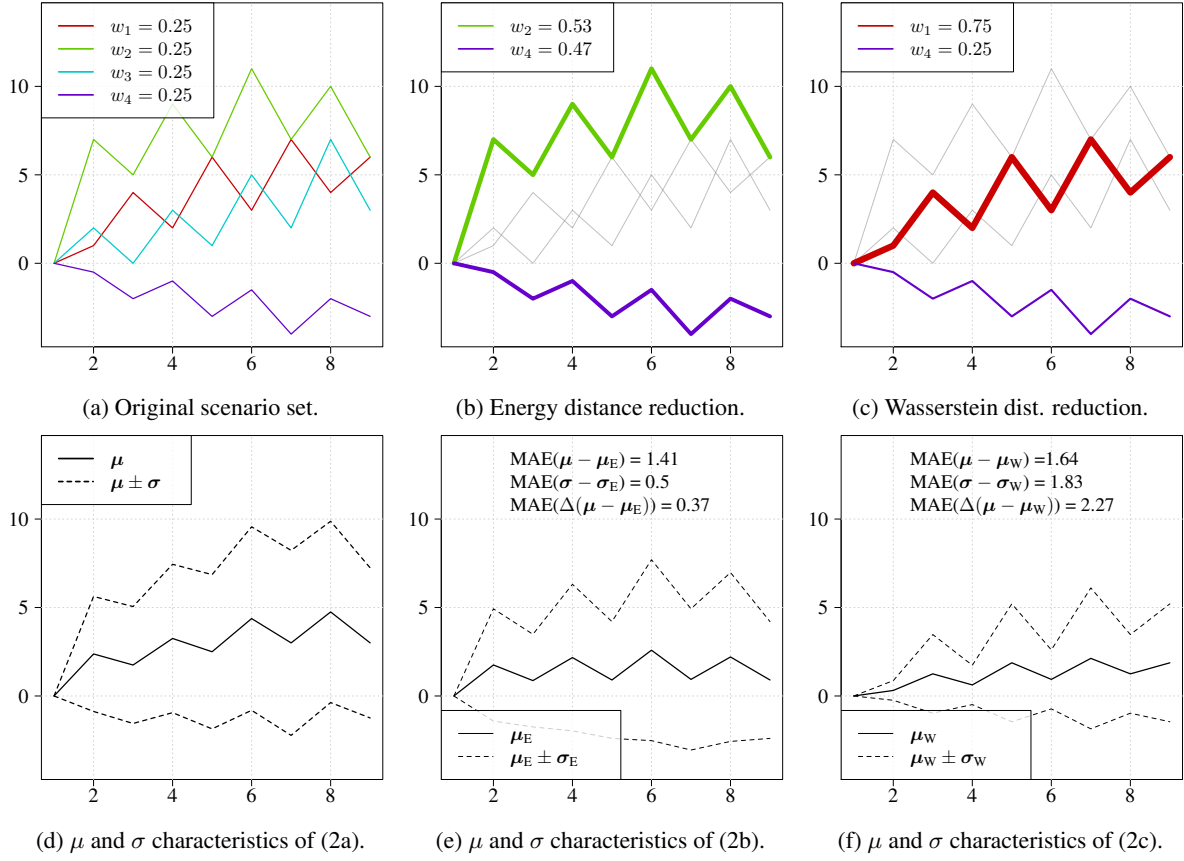


Figure 2: Scenario reduction with 4 equally weighted scenarios which are reduced to 2 scenarios, containing the original setting (left), the reduction for the Energy distance (center) and Wasserstein distance (right). The top row shows the trajectories with corresponding weights. The bottom row illustrates the mean  $\mu = (\mu_1, \dots, \mu_9)$  and the standard deviation  $\sigma = (\sigma_1, \dots, \sigma_9)$  of the full scenario set and the two reductions.

set. Characteristics like the mean and variance structure of the reduced scenario set should match the original data well. A method that transfers the full weight of a removed trajectory fully to another trajectory seems to be suboptimal. Moreover, in Figure 2a we observe that 3 out of 4 trajectories exhibit a zig-zag pattern with positive peaks at even time steps. Thus, the overall mean  $\mu$  in Figure 2d shows the same behavior. Only trajectory 1 (red) deviates from this behavior and shows positive peaks at odd time steps. In the Wasserstein scenario reduction (see 2c) this trajectory 1 (red) got a high weight of 75%. As consequence, the corresponding mean exhibits peaks at odd time steps as well. Thus, this time series characteristic is not covered at all, with likely huge negative consequences in decision making applications.

In contrast, the scenario reduction based on the energy distance (see Figures 2b and 2e) better preserves distributional properties which are usually relevant for decision making. The energy distance method keeps the trajectories 2 (green) and 4 (purple) with non-trivial weight assignment. It notices to some extent that trajectory 1 (red) does not show similar path dependencies to the remaining trajectories and decides for the alternative trajectory 2 (green) as a representative of the three increasing paths. Thus, the original zig-zag pattern of the mean  $\mu$  is preserved in the mean  $\mu_E$  of the reduced scenario set. When comparing quantitative approximation measures, the mean absolute error (MAE) across  $t$ , of  $\mu$ ,  $\sigma$  and  $\Delta\mu = (\mu_1 - \mu_0, \dots, \mu_9 - \mu_8)$  (see Figures 2e and 2f) we notice that in all characteristics, the energy distance based scenario reduction is clearly favorable. Thus, it is worth to further investigate the energy distance for scenario reduction. We restrict ourself to reductions based on probability distances, more detailed on distances for multivariate distribution, sometimes referred to as fan reductions. Most importantly, we ignore nested distance aspects and scenario tree reduction.

In the next section, we introduce the considered setting for ensemble and scenario reduction. In Section 3, we discuss of the energy distance and its properties which we compare with the Wasserstein distance. Afterwards we show applications to a Bernoulli random walk which corresponds to a binary tree and real power system data. We close with a short discussion.

## 2 Basics and notations

Let  $\mathcal{Y} = (\mathbf{y}_i)_{i \in \{1, \dots, n\}} = (\mathbf{y}_1, \dots, \mathbf{y}_n)$  with  $\mathbf{y}_i \in \mathbb{R}^k$  be a set of  $n$   $k$ -dimensional scenarios with associated weights/probabilities  $\mathbf{w} = (w_1, \dots, w_n)$  with  $\mathbf{1}'\mathbf{w} = 1$  and  $w_i \geq 0$ . We may regard  $(\mathcal{Y}, \mathbf{w})$  as weighted ensemble with associated random variable  $\mathbf{Y} = \mathbf{Y}(\mathcal{Y}, \mathbf{w})$  which has the (cumulative) distribution function

$$\mathbf{F}_{\mathbf{Y}}(\mathbf{z}) = \sum_{i=1}^n w_i \mathbb{1}\{\mathbf{y}_i \leq \mathbf{z}\}. \quad (1)$$

In the equally weighted case  $\mathbf{w} = \frac{1}{n}\mathbf{1} = (\frac{1}{n}, \dots, \frac{1}{n})'$ ,  $\mathcal{Y}$  is usually referred to ensemble.

In *weighted ensemble reduction*, we are looking for a suitable subset  $\mathbf{c} = \{c_1, \dots, c_m\} \subseteq \{1, \dots, n\}$  with cardinality  $\#(\mathbf{c}) = m \leq n$  and analyze the reduced subset  $\mathcal{X} = \mathcal{X}(\mathbf{c}) = (\mathbf{x}_i)_{i \in \{1, \dots, m\}} = (\mathbf{y}_i)_{i \in \mathbf{c}} = (\mathbf{y}_{c_1}, \dots, \mathbf{y}_{c_m})$  of  $\mathcal{Y}$  with associated reduced weight vector  $\mathbf{v} = \mathbf{v}(\mathbf{c}; \mathbf{w}) = \frac{1}{s}(w_i)_{i \in \mathbf{c}} = (w_{c_1}, \dots, w_{c_m})/s$  with  $s = \mathbf{1}'(w_i)_{i \in \mathbf{c}}$ . Denote additionally by  $\mathcal{C}_m = \{\mathbf{c} | \mathbf{c} \subseteq \{1, \dots, n\}, \#(\mathbf{c}) = m\}$  the set of all subset of  $\{1, \dots, n\}$  with cardinality  $m$ . The target is now to find  $\mathbf{c} \in \mathcal{C}_m$  so that  $\mathbf{X} = \mathbf{X}(\mathbf{c}) = \mathbf{X}(\mathbf{c}; \mathcal{Y}, \mathbf{w}) \sim \mathbf{F}_{\mathcal{X}}$  with distribution function

$$\mathbf{F}_{\mathbf{X}}(\mathbf{z}) = \sum_{i=1}^m v_i \mathbb{1}\{\mathbf{x}_i \leq \mathbf{z}\} \quad (2)$$

is close to  $\mathbf{Y} \sim \mathbf{F}_{\mathbf{Y}}$  with respect to some distance, see Figure 1a and 1b. If  $\mathbf{w} = \frac{1}{n}\mathbf{1}$  we get  $\mathbf{v} = \frac{1}{m}\mathbf{1}$  and refer this special case as *ensemble reduction* (see Fig. 1a).

Now, let  $d(\cdot, \cdot)$  be a distance between two  $k$ -dimensional random variables. Examples are the Wasserstein and the energy distance which is discussed in more detail in the next section. To recap, the given weighted set of  $n$  scenarios  $(\mathcal{Y}, \mathbf{w})$  is going to be reduced to  $(\mathcal{X}, \mathbf{v}) = ((\mathbf{y}_i)_{i \in \mathbf{c}}, (w_i)_{i \in \mathbf{c}})$  with  $m \leq n$  scenarios corresponding to the subset  $\mathbf{c} \subseteq \{1, \dots, n\}$ . Formally, this reduction problem can be written as a minimization:

$$\mathbf{c}_{\text{opt}}(\mathcal{Y}, \mathbf{w}, m) = \arg \min_{\mathbf{c} \in \mathcal{C}_m} d(\mathbf{X}(\mathbf{c}; \mathcal{Y}, \mathbf{w}), \mathbf{Y}(\mathcal{Y}, \mathbf{w})), \quad (3)$$

with  $\mathbf{X}(\mathbf{c}; \mathcal{Y}, \mathbf{w}) \sim \mathbf{F}_{\mathcal{X}}$  and  $\mathbf{Y}(\mathcal{Y}, \mathbf{w}) \sim \mathbf{F}_{\mathbf{Y}}$  as defined in (2) and (1). Then  $((\mathbf{y}_i)_{i \in \mathbf{c}_{\text{opt}}}, (w_i)_{i \in \mathbf{c}_{\text{opt}}})$  is the optimally reduced ensemble with respect to  $d$ . In general, (3) is an NP-hard problem due to the combinatorial complexity. This means that we can only guarantee to find optimal solutions in low-dimensional cases.

*Scenario reduction* is a generalization of the weighted ensemble reduction. We are looking to the optimal subset  $\mathbf{c} \in \mathcal{C}_m$  with cardinality  $m$  and for optimal weights  $\mathbf{a} = (a_i)_{i \in \mathbf{c}} \in \mathbb{R}^m$ . They are chosen so that the reweighted reduced ensemble  $(\mathcal{X}, \mathbf{a})$  approximates well the original weighted scenario set  $(\mathcal{Y}, \mathbf{w})$  with respect to a distance  $d$  (see Fig. 1c). In general, the scenario reduction problem can be represented as by an inner continuous optimization for the weights  $\mathbf{a}$  and an outer optimization for  $\mathbf{c}$  which corresponds to an integer-valued optimization, see e.g. Römisch (2009); Rujeerapaiboon et al. (2018). Then an optimization procedure for a target reduction size  $m$  can be written as

1. For all  $\mathbf{c} \in \mathcal{C}_m$  solve

$$\mathbf{a}(\mathbf{c}) = \arg \min_{\mathbf{a} \in [0,1]^m, \mathbf{a}' \mathbf{1} = 1} d(\mathbf{X}(\mathbf{c}; \mathcal{Y}, \mathbf{a}), \mathbf{Y}(\mathcal{Y}, \mathbf{w})) \quad (4)$$

with  $\mathbf{X}(\mathbf{c}; \mathcal{Y}, \mathbf{a}) \sim \mathbf{F}_{\mathbf{X}}$  and  $\mathbf{Y}(\mathcal{Y}, \mathbf{w}) \sim \mathbf{F}_{\mathbf{Y}}$  as defined in (2) and (1).

2. Compute

$$\mathbf{c}_{\text{opt}} = \arg \min_{\mathbf{c} \in \mathcal{C}_m} d(\mathbf{X}(\mathbf{c}; \mathcal{Y}, \mathbf{a}(\mathbf{c})), \mathbf{Y}(\mathcal{Y}, \mathbf{w})) \quad (5)$$

and return the optimal solution  $(\mathbf{c}_{\text{opt}}, \mathbf{a}_{\text{opt}}) = (\mathbf{c}_{\text{opt}}, \mathbf{a}(\mathbf{c}_{\text{opt}}))$

As for ensemble reduction,  $\mathcal{C}_m$  is too large to solve the problem by brute force for the majority of practical problems. Note that in general neither (3), nor (4) and (5) do attain a unique minimum. However, in many applications this is usually the case. Still, if the minimum is not unique, we might report and proceed with all minima or use another decision rule to report only one optimum.

### 3 Why the energy distance for reduction problems?

There is a wide range of plausible distances/metrics that measure the discrepancy between two random vectors or two multivariate distributions. Potential candidates are the disparity metric, total variation metric, discrepancy metric, Hellinger distance and Wasserstein distances among others. However, as mentioned in the introduction the Wasserstein metric is by far the most popular for scenario reduction. Hence, we recap its definition on  $\mathbb{R}^k$ :

$$d_{\mathbf{W},p}(\mathbf{X}, \mathbf{Y}) = \left( \inf_{\gamma \in \Gamma(\mathbf{X}, \mathbf{Y})} \int_{\mathbb{R}^k \times \mathbb{R}^k} \|\mathbf{x} - \mathbf{y}\|_2^p d\gamma(\mathbf{x}, \mathbf{y}) \right)^{\frac{1}{p}} \quad (6)$$

where  $\Gamma(\mathbf{X}, \mathbf{Y})$  is the set of all probability measures on  $\mathbb{R}^k \times \mathbb{R}^k$  with the same marginals as  $\mathbf{X}$  on the first  $k$  coordinates and the same as  $\mathbf{Y}$  on the latter ones.  $\Gamma(\mathbf{X}, \mathbf{Y})$  is also known as set of  $\mathbf{X}$  and  $\mathbf{Y}$  couplings. As mentioned in the introduction, the popularity of the Wasserstein distance in scenario reduction is mainly due to available stability results for the Wasserstein distance in stochastic programming Römisch (2003) and the efficient reduction algorithm, see Dupačová et al. (2003); Römisch (2009). The latter provides an efficient and explicit formula for the subproblem (4) in scenario reduction. The resulting optimal redistribution rule (see e.g. Growe-Kuska et al. (2003)) corresponds to a (mass) transportation problem. Here, it is important to remark that this algorithm does not require the explicit computation of the Wasserstein distance, which leads to a dramatic speed up compared to alternatives.

Still, even for Wasserstein based scenario reduction, the NP-hard integer-valued optimization problem (5) is remaining. Thus, in ensemble reduction (3) the advantages of the Wasserstein distance diminish as the inner optimization step in (4) is not required.

The NP-hard integer-valued subproblem (3) or (4) is usually solved by heuristics for higher dimensional problems. Typically, forward selection (FS), backward selection (BS) or similar algorithms like fast forward selection (FFS) or forward selection in wait-and-see clusters (FSWC) are applied, see e.g. Growe-Kuska et al. (2003); Römisch (2009); Feng and Ryan (2013). However, other alternatives like particle swarm optimization, neural network bases on deep learning methods and other heuristics are applied as well, see Li and Gao (2019).

The Wasserstein distance  $d_{\mathbf{W},1}$  with  $p = 1$  is often applied to scenario reduction as it satisfies the duality theorem of Kantorovich and Rubinstein. Also note that in the  $k = 1$ -dimensional case, the Wasserstein distance satisfies  $d_{\mathbf{W},p}(\mathbf{X}, \mathbf{Y}) = \|F_{\mathbf{X}}^{-1} - F_{\mathbf{Y}}^{-1}\|_p$ , see e.g. Pflug and Pichler (2014). Thus,  $d_{\mathbf{W},1}$  simplifies to

$$d_{\mathbf{W},1}(\mathbf{X}, \mathbf{Y}) = \int_{\mathbb{R}} |F_{\mathbf{X}}(z) - F_{\mathbf{Y}}(z)| dz, \quad (7)$$

which is the  $L^1$ -distance between the two cumulative distribution functions.

A related discrepancy measure to (7) is the Cramér distance. It is given by

$$d_C(\mathbf{X}, \mathbf{Y}) = \int_{\mathbb{R}} |F_{\mathbf{X}}(z) - F_{\mathbf{Y}}(z)|^2 dz \quad (8)$$

and measures the squared  $L^2$ -distance between the two cumulative distribution functions. Thus, just from the intuitive point of view  $d_{\mathbf{W},1}$  and  $d_C$  should exhibit similar properties. The Cramér distance has a useful different representation given by

$$d_C(\mathbf{X}, \mathbf{Y}) = \mathbb{E}|X - Y| - \frac{1}{2}\mathbb{E}|X - X'| - \frac{1}{2}\mathbb{E}|Y - Y'|, \quad (9)$$

where  $X'$  and  $Y'$  are iid copies of  $X$  and  $Y$ .

Now, the interesting part is that the representation (9) allows for a natural generalization of the Cramér distance to  $\mathbb{R}^k$ , called energy distance, see Székely and Rizzo (2013). The *energy distance* is defined as

$$d_{E,p}(X, Y) = \mathbb{E}\|X - Y\|_2^p - \frac{1}{2}\mathbb{E}\|X - X'\|_2^p - \frac{1}{2}\mathbb{E}\|Y - Y'\|_2^p \quad (10)$$

where  $p \in (0, 2)$  and again  $X'$  and  $Y'$  are an iid copy of  $X$  and  $Y$ . Obviously, for  $k = 1$  and  $p = 1$  (10) corresponds to the Cramér distance. The case  $p = 1$  is regarded as the standard energy distance for  $k > 1$ . Moreover, the energy distance is a special case of the maximum mean discrepancy (MMD), see e.g. Borgwardt et al. (2006).

As pointed out in Székely and Rizzo (2013); Székely and Rizzo (2017), the energy distance satisfies all axioms of a metric, especially that the energy distance is zero ( $d_{E,p}(X, Y) = 0$ ) if and only if  $X$  and  $Y$  share the same distribution (almost surely). Moreover, it has useful transformation properties. So  $d_{E,p}$  is scale equivariant, i.e. for all constants  $a \in \mathbb{R}$  there is a non-zero real-valued function  $g$  such that it holds  $d_{E,p}(aX, aY) = g(a)d_{E,p}(X, Y)$ . The energy distance satisfies the condition by choosing  $g(z) = z^p$ , which makes the choice  $p = 1$  to a natural candidate for applications. Furthermore, the energy distance exhibits rotational invariance, i.e. for every orthonormal matrix  $A$  it holds  $d_{E,p}(AX, AY) = d_{E,p}(X, Y)$ . It is interesting to note, that the multivariate version of (8) results in a measure that is not rotational invariant. This is a hint that (9) is more suitable for a  $k$ -dimensional generalizations than (8) which focuses on the distances between the cumulative distribution functions. It also indicates that in higher dimensions the properties of the Wasserstein distance might deviate substantially from the energy distance. Moreover, we want to remark that also the Wasserstein distance is scale and rotational invariant. It holds  $d_{W,p}(aX, aY) = |a|d_{W,p}(X, Y)$  and  $d_{W,p}(AX, AY) = d_{W,p}(X, Y)$  for all  $p$ , see Muskulus and Verduyn-Lunel (2011).

The probably most important property of the energy distance is an alternative representation by characteristic functions. The energy distance can be rewritten as a weighted  $L^2$ -distance of the characteristic functions  $\varphi_X$  and  $\varphi_Y$  with  $\varphi_X(z) = \mathbb{E}(e^{iz'X})$  and  $\varphi_Y(z) = \mathbb{E}(e^{iz'Y})$ :

$$d_{E,p}(X, Y) = C_{k,p} \int_{\mathbb{R}^k} \frac{|\varphi_X(z) - \varphi_Y(z)|^2}{\|z\|_2^{k+p}} dz \quad \text{with} \quad C_{k,p} = \frac{\pi^{\frac{k}{2}} \Gamma(1 - \frac{p}{2})}{p 2^p \Gamma(\frac{k+p}{2})} \quad (11)$$

Here,  $C_{k,p}$  is a scaling constant which depends only on the dimension  $k$  and  $p$ . The weight function  $\xi(z) = \|z\|_2^{-(k+p)}$  is a polynomial of the Euclidean norm depending on the dimension  $k$ . Interestingly, this is the only choice of any continuous function  $\xi$  such that for some  $C > 0$  the weighted  $L^2$ -distance  $C \int_{\mathbb{R}^k} \xi(z) |\varphi_X(z) - \varphi_Y(z)|^2 dz$  between the characteristic functions  $\varphi_X$  and  $\varphi_Y$  is scale equivariant and rotational invariant.

The characterization by characteristic functions allows the energy distance to serve for powerful tests and the characterization of independence, see Rizzo and Székely (2016). For instance Székely and Rizzo (2013) show that the energy distance based test for multivariate normality has a high testing power, higher than all commonly used alternatives. Moreover, it can be utilized to test for non-parametric characteristics like symmetry or skewness. The other very crucial feature is that the energy distance allows the construction of the distance covariance and joint distance covariance, Chakraborty and Zhang (2019). Those dependency measures can be used to construct tests for multivariate independence, which is remarkable on its own. According to Chakraborty and Zhang (2019), this is the only known scale and rotation invariant way to test for multivariate independence. As we want to maintain the dependency structure in the scenario paths properly the energy distance serves as a suitable candidate for reduction problems.

In general, the considered distances for reduction problems have to be computed. This holds always for the energy distance  $d_{E,p}$  and in ensemble reduction also for the Wasserstein distance  $d_{W,p}$ . The Wasserstein distance can be computed by minimum matching and solving the linear programming Nguyen (2011)

$$d_{W,p}(X, Y) = \min_{q \in [0,1]^{\{1,\dots,n\} \times c}} \left( \sum_{(i,j) \in \{1,\dots,n\} \times c} q_{i,j} \|y_i - y_j\|_2^p \right)^{1/p} \quad (12)$$

such that  $\sum_{i=1}^n q_{i,j} = w_j$  and  $\sum_{j \in c} q_{i,j} = w_i$ . This problem can be solved using standard linear program methods. Gottschlich and Schuhmacher (2014) propose an alternative shortlist method for (12) which is based on the simplex algorithm and allows substantial speed improvements for multiple applications. The energy distance  $d_{E,p}$  (10) can be calculated by equation:

$$\begin{aligned} d_{E,p}(X, Y) &= \frac{1}{nm} \sum_{i=1}^n \sum_{j \in c} \|w_i y_i - w_j y_j\|_2^p \\ &\quad - \frac{1}{2m^2} \sum_{i \in c} \sum_{j \in c} \|w_i y_i - w_j y_j\|_2^p - \frac{1}{2n^2} \sum_{i=1}^n \sum_{i=1}^n \|w_i y_i - w_j y_j\|_2^p. \end{aligned} \quad (13)$$

However, in reduction problems we do not have to compute equation (13), as the latter term remains unchanged for all  $\mathbf{c}$ . Thus, it is sufficient to replace  $d_{E,p}$  by

$$\text{ES}_p(\mathbf{X}, \mathbf{Y}) = \frac{1}{nm} \sum_{i=1}^n \sum_{j \in \mathbf{c}} \|w_i \mathbf{y}_i - w_j \mathbf{y}_j\|_2^p - \frac{1}{2m^2} \sum_{k \in \mathbf{c}} \sum_{j \in \mathbf{c}} \|w_j \mathbf{y}_j - w_k \mathbf{y}_k\|_2^p \quad (14)$$

which is known as the *energy score* which is popular in forecasting evaluation, see Gneiting and Raftery (2007). In forecast evaluation, usually one-sided measures are required. So one input is taken as random variable, the other input is treated as observation in  $\mathbb{R}^k$  and as already materialized. Among forecasters the continuous ranked probability score (CRPS) is usually regarded as the suitable 1-dimensional forecasting criterion for distributions. The CRPS is the one-sided counterpart of the Cramér distance (9). Concerning the computation of the energy score, we remark that the computational complexity for calculating the terms  $\|w_i \mathbf{y}_i - w_j \mathbf{y}_j\|_2^p$  for all  $i$  and  $j$  is fast and of order  $O(nm)$ .

For scenario reduction, the Wasserstein based approaches have the speed advantage due to the mentioned explicit algorithm proposed by Dupačová et al. (2003). In these cases, the energy distance based method have a speed disadvantage. However, the inner optimization step in (4) turns with (14) to

$$\mathbf{a}(\mathbf{c}) = \arg \min_{\mathbf{a} \in [0,1]^m, \mathbf{a}' \mathbf{1} = 1} \text{ES}_p(\mathbf{X}(\mathbf{c}; \mathcal{Y}, \mathbf{a}), \mathbf{Y}(\mathcal{Y}, \mathbf{w})) \quad (15)$$

$$= \arg \min_{\mathbf{a} \in [0,1]^m, \mathbf{a}' \mathbf{1} = 1} \frac{1}{nm} \sum_{i=1}^n \sum_{j \in \mathbf{c}} \|a_i \mathbf{y}_i - w_j \mathbf{y}_j\|_2^p - \frac{1}{2m^2} \sum_{i \in \mathbf{c}} \sum_{j \in \mathbf{c}} \|a_i \mathbf{y}_i - a_j \mathbf{y}_j\|_2^p, \quad (16)$$

which is a quadratic program (QP) with linear constraints. There is plenty of literature available to solve quadratic optimizations, Bao et al. (2011). In general, the matrix  $\mathbf{A} = (a_{i,j})_{(i,j) \in \mathbf{c} \times \mathbf{c}}$  is indefinite. Thus, we are facing the most complicated QP which might be potentially NP-hard, see Vavasis (1992).

However, our empirical applications show that standard algorithms provide a solution in reasonable time. The reason is likely the very special structure of  $\mathbf{A}$  which is a Euclidian distance matrix (EDM) and is mainly studied in the context of Euclidean distance matrix completion problems (EDMCP). Such a matrix has full rank if  $\mathbf{y}_i \neq \mathbf{y}_j$  for all  $i, j \in \mathbf{c}$  with  $i \neq j$ , Ball (1992). Additionally, Hayden and Tarazaga (1993) provides a proof that  $-\mathbf{A}$  has exactly one negative eigenvalue. As our feasible region of the QP is compact, we can apply quadratic programming theory (see Vavasis (1992)). It follows that there exists a polynomial time algorithm for (16) that provides  $\varepsilon$ -exact solutions. As  $-\mathbf{A}$  has exactly one negative eigenvalue, this polynomial time is in fact quadratic. However, to our knowledge there is no algorithm for QPs with EDMs available so far where this property has been proven. Still, it is fair to assume that any reasonable algorithm available for solving (16) will benefit from the aforementioned structure of the problem.

## 4 Applications

In this section, we show different applications for ensemble and scenario reduction using the energy distance and the Wasserstein distance for comparison purpose. First we study ensemble and scenario reduction for a Bernoulli random walk which corresponds to a binary tree. Afterwards, we consider scenario reduction for electricity load/demand/consumption and electricity prices<sup>2</sup>, which are highly relevant in many energy systems applications. However, both considered real data studies are mainly for illustration purpose. We do not apply the reduced scenario sets in a subsequent optimization problem.

### 4.1 Bernoulli random walk

We consider a symmetric Bernoulli random walk (also called symmetric simple random walk and coin-tossing random walk), where  $P[Y_t = Y_{t-1} - 1] = P[Y_t = Y_{t-1} + 1] = 0.5$  with  $Y_0 = 0$ . The resulting paths correspond to an equally weighted binary tree which branches every step by  $-1$  and  $1$ . We consider  $T = 5$  time steps to keep the problem sufficiently small and allow for the computation of exact solutions. The resulting  $n = 2^T = 2^5 = 32$  paths in the scenario set are interpreted as a fan, not as a tree. Note that we ignore additional information due to the tree structure which could be included into the reduction technique by considering nested distances, see e.g. Pflug and Pichler (2014).

We apply exact ensemble and scenario reduction to reduce the number of trajectories from  $n = 32$  to  $m \in \{2, \dots, 5\}$  with respect to the energy distance  $d_{E,1}$  and the Wasserstein distance  $d_{W,1}$ . Note that due to the symmetry the resulting solutions are usually not unique. Thus, we report only one optimal solution. Figures 3 and 4 show the results for the ensemble and scenario reduction problem. They also provide the optimal trajectories and for the scenario reduction problem the resulting weights. Similarly to the Figure 2 in the introduction, we also report

<sup>2</sup>The considered data is available at <https://transparency.entsoe.eu>

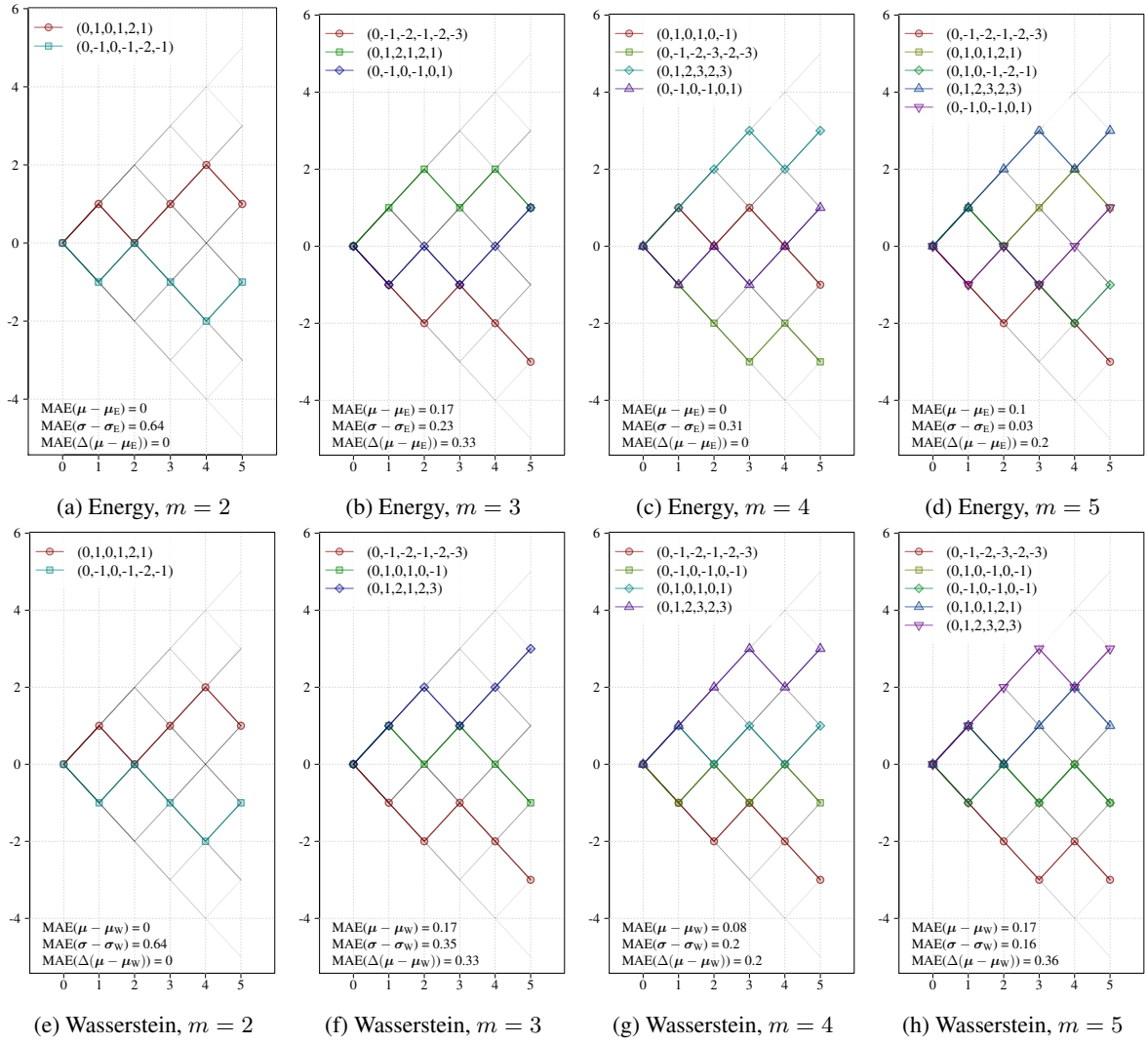


Figure 3: Exact ensemble reduction for a symmetric Bernoulli random walk of size  $T = 5$  and  $n = 2^T = 32$  scenarios. The reduction solutions is performed for  $m = 2, \dots, 5$  scenarios (from left to right) for the energy distance  $d_{E,1}$  (top row) and the Wasserstein distance  $d_{W,1}$  (bottom row). The resulting trajectories (top legends) the MAE of the approximation of  $\mu_t$ ,  $\sigma_t$  and  $\Delta\mu_t$  are shown (bottom legends).

key characteristics for the approximation of the reduced scenario set to the original set of  $n = 32$  paths. In detail, we report again the mean absolute error (MAE) of the approximation for the mean  $\mu = (\mu_0, \dots, \mu_5)$ , standard deviation  $\sigma = (\sigma_0, \dots, \sigma_5)$  and difference of the mean  $\Delta\mu = (\mu_1 - \mu_0, \dots, \mu_5 - \mu_4)$ .

In Figures 3 and 4, we observe that for  $m = 2$  both distances lead to the same optimal solution. However, for  $m > 2$  the solutions of the energy distance and the Wasserstein distance deviate for both the ensemble reduction problem and the scenario reduction problem. For ensemble reduction and  $m = 3$  (Fig. 3b and 3f), we see that both solutions have the same MAE performance for the mean approximation but the energy distance approximates better the variance structure. For  $m = 4$  (Fig. 3c and 3g), the results are mixed. The energy distance reduction maintains perfectly the mean behavior in contrast to the Wasserstein distance. But this comes at the cost of a worse explanation of the variance structure. For  $m = 5$  (Fig. 3d and 3h), the picture is clear. The energy distance has a better approximation in all considered characteristics. Another fact that can be observed for  $m = 5$  is that in the last step from  $t = 4$  to  $t = 5$ , the energy distance captures better the path dependency than the Wasserstein distance. In a binary tree, the ratio of branches which go upwards and downwards is equally distributed. As  $m = 5$  is odd this can never be perfectly captured in ensemble reduction. The energy distance reduction selects three increasing and two decreasing paths from  $t = 4$  to  $t = 5$ . On the other hand, the optimal Wasserstein distance reduction provides one increasing trajectory and four decreasing trajectories which is an unnecessary bias from the true behavior.

For the scenario reduction (Fig. 4) with  $m > 2$  the quantitative measures are even more in favor for the energy distance. Here, in all characteristics the energy distance reduction obtains preferable results. Moreover, we notice that the weights (Fig. 4b, 4c and 4d) of the energy distance are more equally distributed among all paths than for the Wasserstein distance (Fig. 4f, 4g and 4h). This is not automatically an advantage. However, it indicates that the



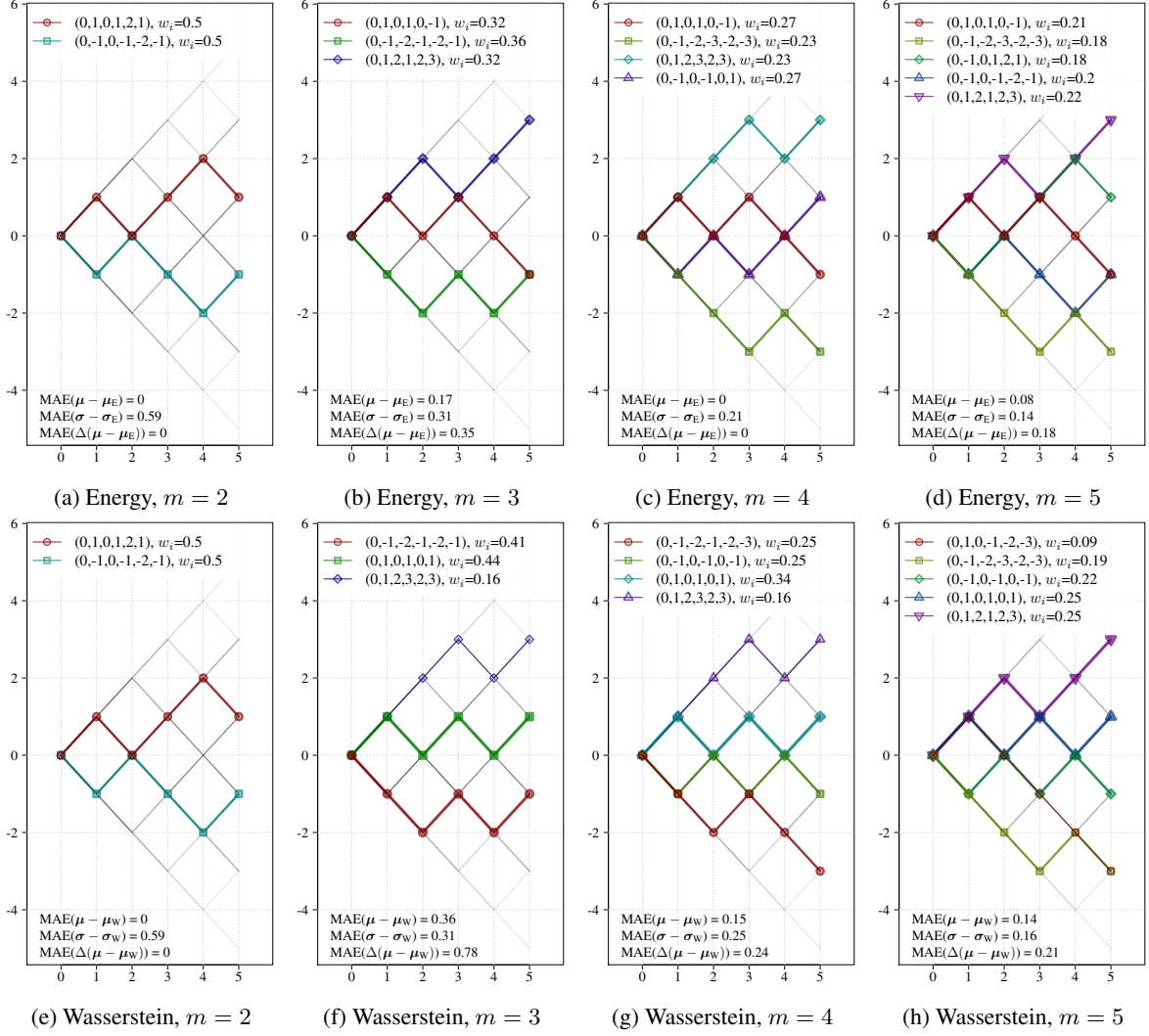


Figure 4: Exact scenario reduction for a symmetric Bernoulli random walk of size  $T = 5$  and  $n = 2^T = 32$  scenarios. The reduction solutions is performed for  $m = 2, \dots, 5$  scenarios (from left to right) for the energy distance  $d_{E,1}$  (top row) and the Wasserstein distance  $d_{W,1}$  (bottom row). The resulting trajectories and weights (top legends) the MAE of the approximation of  $\mu_t$ ,  $\sigma_t$  and  $\Delta\mu_t$  are shown (bottom legends).

energy score potentially mixes the scenario properties in a stronger way as the weights are closer to the uniform distribution which corresponds to maximum entropy.

## 4.2 Electricity load profiles

We consider quarter-hourly German electricity demand data in two different scenario reduction settings. The first application is a small reduction problem where we can consider exact reduction methods. The second application uses forward selection for the scenario reduction and illustrates some reduction characteristics. In the first case, we apply scenario reduction using the energy distance  $d_{E,1}$  and the Wasserstein distance  $d_{W,1}$ . In the second example, we extend the set of considered distances to  $d_{E,p}$  with  $p \in \{0.5, 1, 2\}$  and  $d_{W,p}$  with  $p \in \{1, 2, 3\}$  to evaluate the impact of  $p$ .

### 4.2.1 Exact reduction for demand profiles of 3rd Wednesday of each month.

This example considers electricity load data from January 2017 to December 2019. For each month the load profile of every 3rd Wednesday of each month is considered as the scenario set. This gives us  $n = 3 \times 12 = 36$  historic demand trajectories in total. Thus, exact scenario reduction is computationally feasible, at least for some settings with small  $m$ . The consideration of every third 3rd Wednesday in month is sometimes considered in power systems literature as well, see e.g. Andrychowicz et al. (2017). The considered data and overall reduction results for  $m = 2, \dots, 5$  are given in Figure 5. Figures 5a and 5b depict the 36 path for the scenario reduction problem and the mean and variance characteristics. Figure 5c to Figure 5j show the results of exact scenario reduction for the energy distance  $d_{E,1}$  and Wasserstein distance  $d_{W,1}$  with the same MAE output measure as used before.

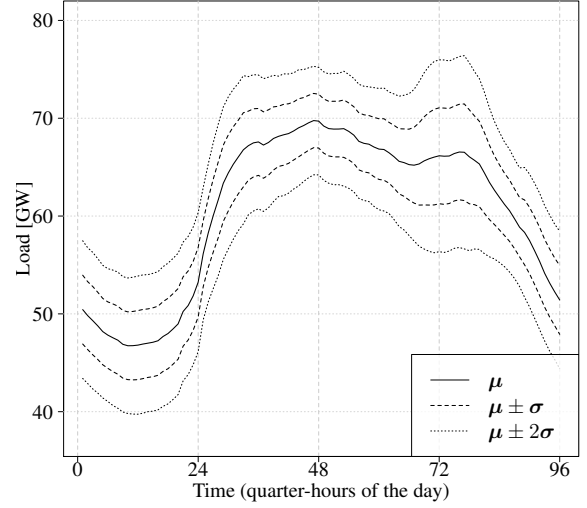
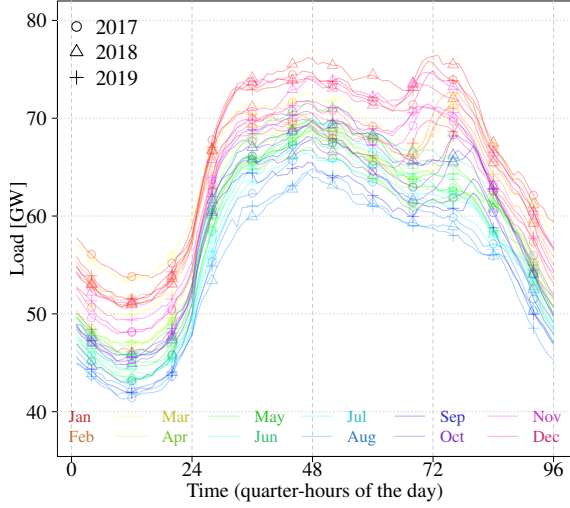
We observe that the overall behavior is similarly to Bernoulli random walk example but less clear in favor for the energy distance. The energy distance reduction results tend to have a superior behavior concerning the mean properties. Concerning the approximation of the correct variance structure, the results are mixed. For  $m = 2$  and  $m = 3$ , the Wasserstein distance covers the true variance pattern slightly better than the energy distance reduction. Vice versa for  $m = 4$  and  $m = 5$ , where the energy distance has preferable variance behavior. Again, we see that the weights of the energy distance reduction are more equally distributed. For instance for  $m = 4$  (Figures 5e and 5i), the Wasserstein distance has a maximum weight of 0.47 for the May'19 trajectory and a minimum weight of 0.14 for the Jan'19 trajectory. In contrast, the energy distance reduction leads to a maximum and minimum weight of 0.30 and 0.21. Thus, we expect more stable and better mixed results from energy distance reductions. Further, we observe that the Wasserstein distance reduction has the tendency to choose slightly more extreme trajectories. Consider e.g.  $m = 4$ : The Wasserstein distance selected Aug'17 as representative summer trajectory. However, this Aug'17 trajectory has the lowest night load among all considered trajectories in the scenario set. The energy distance selects the Jul'19 path for the representative summer trajectory. This has a slightly higher overall demand level, also during the night hours. For  $m = 3$ , we observe a similar selection pattern. The energy distance chooses Dec'18 as representative winter trajectory whereas the Wasserstein distance selects the Jan'19. The latter has a more distinct evening peak.

### 4.2.2 Forward reduction for demand profiles.

In this larger scenario reduction, application we consider all daily electricity load profiles from 2019 as set of original trajectories. The  $n = 365$  trajectories are reduced to  $m = 2, \dots, 100$  scenarios. As exact reduction is computationally not feasible, we consider forward selection, see e.g. Heitsch and Römis (2007). We use simple 1-step forward selection where we add in every iteration one trajectory to the scenario set. This, allows us to compare properties of the reduced set of trajectories with respect to the energy and Wasserstein distance, where we first focus on  $d_{E,1}$  and  $d_{W,1}$ .

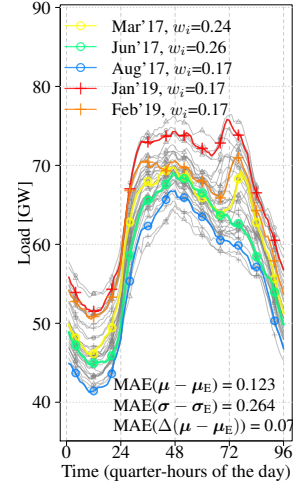
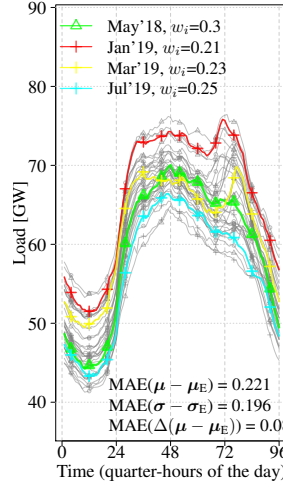
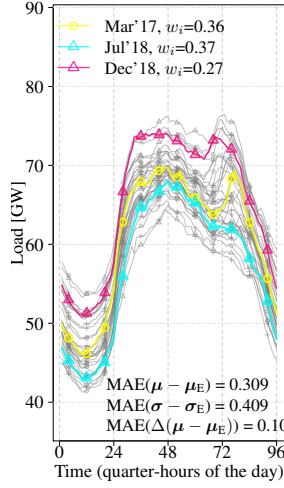
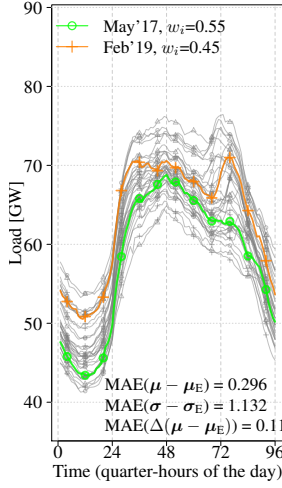
Figure 6 presents the setting and the results of the reduction task. The top row (Figures 6a and 6b) illustrate the original set of 365 trajectories with mean and variance characteristics. Figures 6c and 6d depict the scenario reduction results for the energy and Wasserstein distance for  $m = 10$  final scenarios. They also include the final weights and MAE approximation errors of  $\mu_t$ ,  $\sigma_t$  and  $\Delta\mu_t$ . Additionally, Figures (7a), (7b) and (7c) depict the three MAE errors for all considered scenario reduction sizes up to  $m = 100$ . Due to the high variations of the MAEs with respect to  $m$ , we added a monotonic smoothing spline fit to allow for better interpretation.

First, we interpret the results for  $m = 10$  (see 6c and 6d). We observe that the results are similar to the exact reduction results we have seen before. The energy distance seems to provide more equally distributed weights for each trajectory than the Wasserstein distance. The weights vary between 0.087 and 0.121 whereas the Wasserstein distance weights vary between 0.060 and 0.170. Thus, the spread is more than 3 times as high. Moreover, we observe that both methods provide 10 trajectories that cover the general behavior of the data. They include working days and weekend days, such as days in summer and winter. Still, again the energy distance seems to spread the annual characteristic in a better way. As we apply forward selection we might also interpret the order of the considered trajectories. We see that both algorithm choose in the first step the same trajectory from Tue 28May but deviate from the second step onwards. A plausible result is that both algorithms choose a weekend day as second



(a) Considered scenarios

(b) Mean and Variance characteristics of (5a)

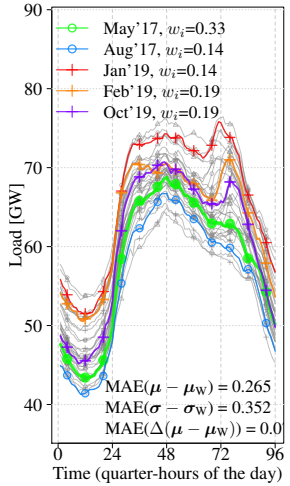
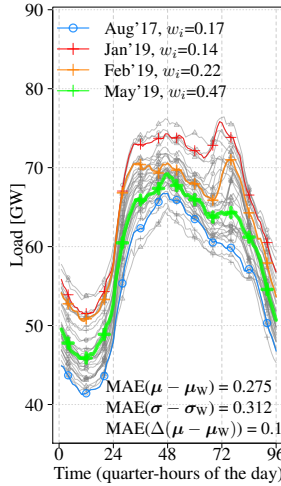
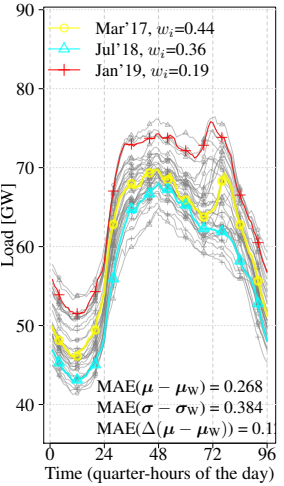
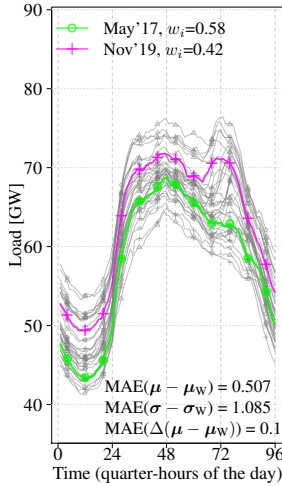


(c) Energy,  $m = 2$

(d) Energy,  $m = 3$

(e) Energy,  $m = 4$

(f) Energy,  $m = 5$



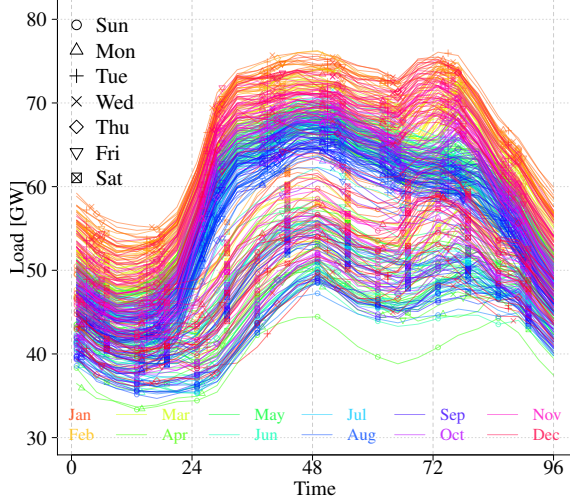
(g) Wasserstein,  $m = 2$

(h) Wasserstein,  $m = 3$

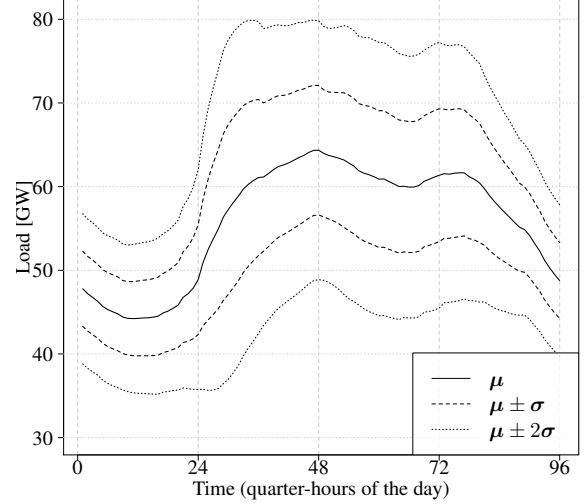
(i) Wasserstein,  $m = 4$

(j) Wasserstein,  $m = 5$

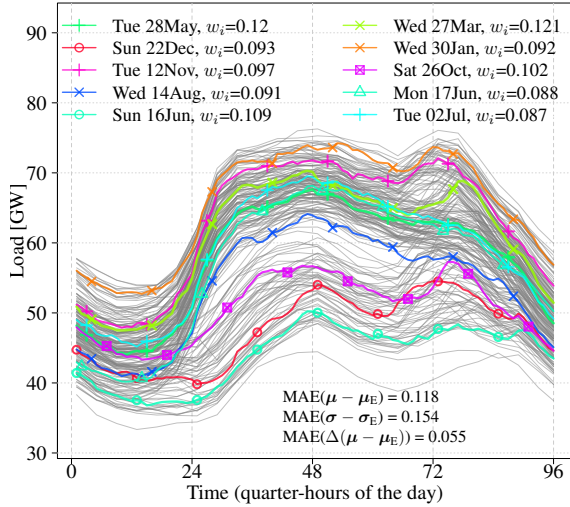
Figure 5: Exact scenario reduction for demand profiles with  $n = 36$  scenarios. The top row shows the  $n = 36$  scenarios (top left) with expected value and standard deviation characteristics (top right). The reduction solutions is performed for  $m = 2, \dots, 5$  scenarios (from left to right, center and bottom) for the energy distance  $d_{E,1}$  (center row) and the Wasserstein distance  $d_{W,1}$  (bottom row). The resulting trajectories and weights (top legends) the MAE of the approximation of  $\mu_t$ ,  $\sigma_t$  and  $\Delta\mu_t$  are shown (bottom legends).



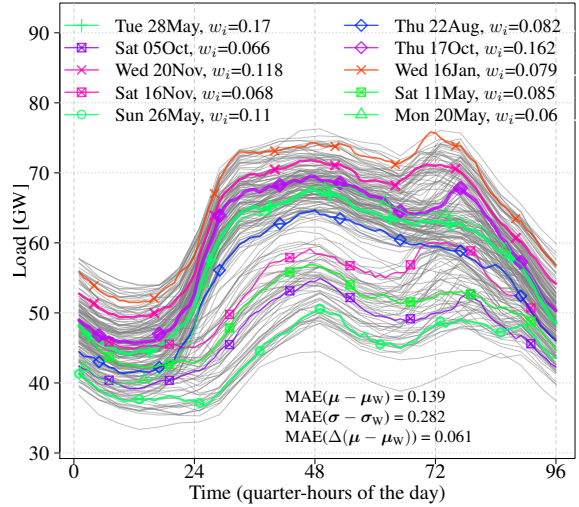
(a) Considered scenarios



(b) Mean and Variance characteristics of (6a)



(c) Reduction using the energy distance



(d) Reduction using the Wasserstein distance

Figure 6: Scenario reduction using forward selection for demand profiles with  $n = 365$  scenarios. The top row shows the  $n = 365$  scenarios (top left) with expected value and standard deviation characteristics (top right). The reduction solutions for  $m = 10$  scenarios for the energy distance  $d_{E,1}$  (center left) and the Wasserstein distance  $d_{W,1}$  (center right) with characteristics.

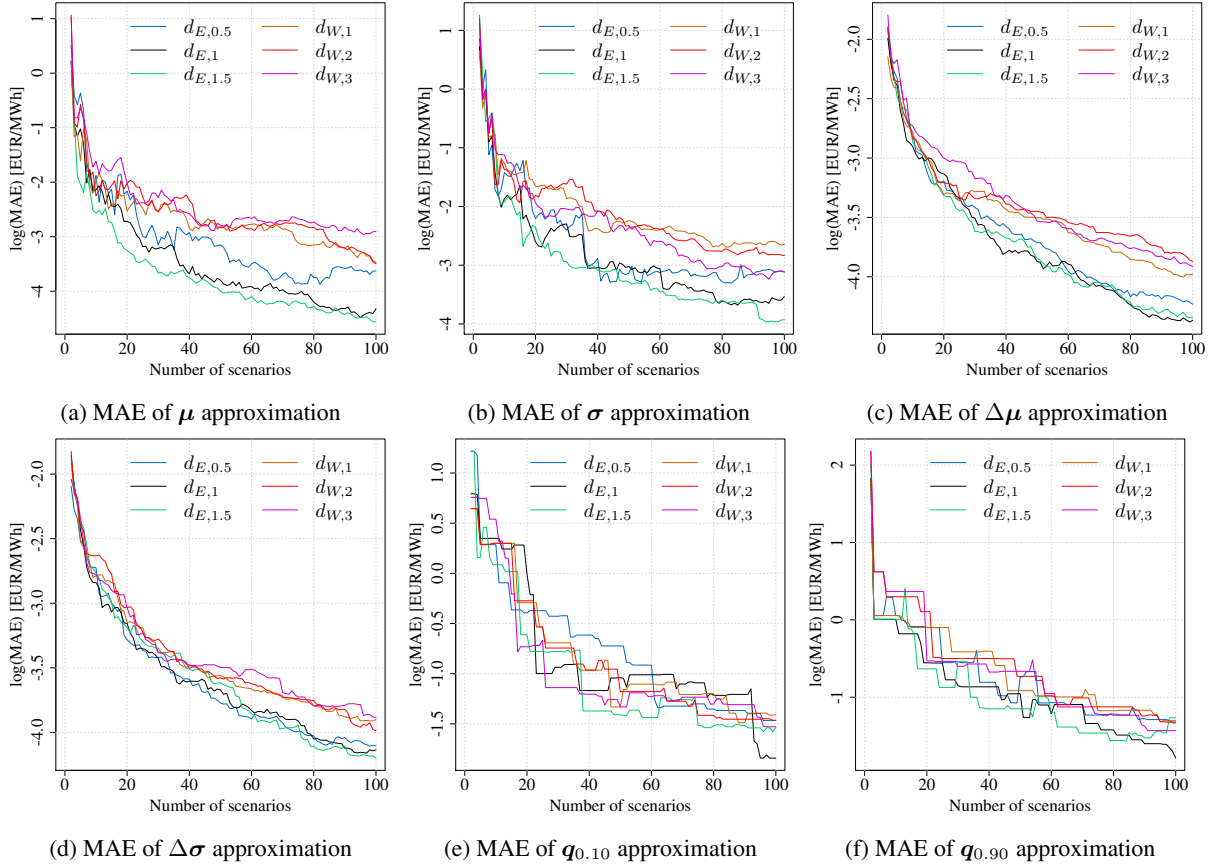


Figure 7: Scenario reduction results by the energy distances ( $d_{E,0.5}$ ,  $d_{E,1}$ ,  $d_{E,1.5}$ ) and Wasserstein distances ( $d_{W,1}$ ,  $d_{W,2}$ ,  $d_{W,3}$ ). It shows the approximation accuracy in logarithm of the MAE (mean absolute error) of  $\mu$  (top left),  $\sigma$  (top center),  $\Delta\mu$  (top right),  $\Delta\sigma$  (bottom left), 10%-quantile  $q_{0.10}$  (bottom center) and 90%-quantile  $q_{0.90}$  (bottom right) for  $m = 2, \dots, 100$  scenarios of the  $n = 365$  scenarios.

trajectory. Concerning the overall weekend representation, the energy distance reduction chooses a winter Sunday, a summer Sunday and a fall Saturday whereas the Wasserstein based reduction chooses two fall Saturdays, a spring Saturday and a spring Sunday. Again, the energy distance results seem to be more dispersed. The provided MAE values draw the same picture: The energy distance provides better mean and variance approximations.

Now we turn towards the results of the MAE measures for different reduction sizes  $m$ . They are provided in Figure 7 for  $d_{E,0.5}$ ,  $d_{E,1}$ ,  $d_{E,1.5}$ ,  $d_{W,1}$ ,  $d_{W,2}$  and  $d_{W,3}$ . Next to the mean approximation ( $\mu = (\mu_1, \dots, \mu_{96})$ ), the standard deviation  $\sigma = (\sigma_1, \dots, \sigma_{96})$  and the mean difference ( $\Delta\mu = (\mu_2 - \mu_1, \dots, \mu_{96} - \mu_{95})$ ) we consider also the standard deviation difference ( $\Delta\sigma = (\sigma_2 - \sigma_1, \dots, \sigma_{96} - \sigma_{95})$ ) and the 10%- and 90%-quantile processes ( $q_{0.10} = (q_{0.10,1}, \dots, q_{0.10,96})$  and  $q_{0.90} = (q_{0.90,1}, \dots, q_{0.90,96})$ ). First, we see that all approximations tend to get better when the number of scenarios increases. All energy distances show better mean and variance statistics (see 7a, 7b, 7c, 7d) than the Wasserstein distances. For the 10% and 90% quantiles (see 7e, 7f), this is not the case. Here, no distance is clearly preferable. Among the considered energy distances,  $d_{E,p}$  tends to have slightly better results for the mean and variance approximations for larger  $p$ .

### 4.3 Scenario reduction for electricity prices.

In this final example we want to show an illustration for a larger real data set that is more heavy tailed and thus sensitive to outliers. Therefore, we consider 10 years of recent hourly German day-ahead electricity spot price profiles, from 01.07.2010 to 30.06.2020. Table 1 shows some summary statistics of the considered data set and their first difference. We observe that the data set contains some positive and negative price spikes indicated by the large (in absolute terms) minimum and maximum, characteristic for electricity price data, see Ziel and Steinert (2018). We reduce the  $n = 3653$  daily profile trajectories  $y_i = (y_{i,1}, \dots, y_{i,24})$  with  $i \in \{1, \dots, n\}$  for the energy and Wasserstein distance by evaluating additionally the impact of the parameter  $p$  in both definitions by evaluating again  $d_{E,0.5}$ ,  $d_{E,1}$ ,  $d_{E,1.5}$ ,  $d_{W,1}$ ,  $d_{W,2}$  and  $d_{W,3}$ . As for the load profile, we consider a 1-step forward selection as reduction algorithm.

We conduct the scenario reduction for a scenario size of  $m = 2, \dots, 100$  and evaluate the approximation accuracy of specific characteristics. We consider as before the mean ( $\mu = (\mu_1, \dots, \mu_{24})$ ), the standard deviation  $\sigma = (\sigma_1, \dots, \sigma_{24})$ , difference in  $\mu$  and  $\sigma$  ( $\Delta\mu = (\mu_2 - \mu_1, \dots, \mu_{24} - \mu_{23})$ ,  $\Delta\sigma = (\sigma_2 - \sigma_1, \dots, \sigma_{24} - \sigma_{23})$ ), and



	$\mu$	$\sigma$	min	max	$q_{0.10}$	$q_{0.25}$	$q_{0.50}$	$q_{0.75}$	$q_{0.90}$	$\rho$	$\gamma$	$\kappa$
$\mathbf{y}_i$	37.68	17.08	-221.99	210.00	18.77	27.96	36.93	47.95	58.43	0.74	-0.51	11.76
$\Delta \mathbf{y}_i$	0.11	5.64	-102.76	156.94	-5.28	-2.36	-0.20	2.20	6.20	-0.03	0.92	33.40

Table 1: Summary statistics of electricity price data  $\mathbf{y}_1, \dots, \mathbf{y}_{3653}$ : mean ( $\mu$ ), standard deviation ( $\sigma$ ), minimum (min), maximum (max), quantiles for 10%, 25%, 50%, 75%, 90% ( $q_{0.10}, q_{0.25}, q_{0.50}, q_{0.75}, q_{0.90}$ ), mean correlation ( $\rho$ ), skewness ( $\gamma$ ) and kurtosis ( $\kappa$ ) across all  $n = 3653$  trajectories.

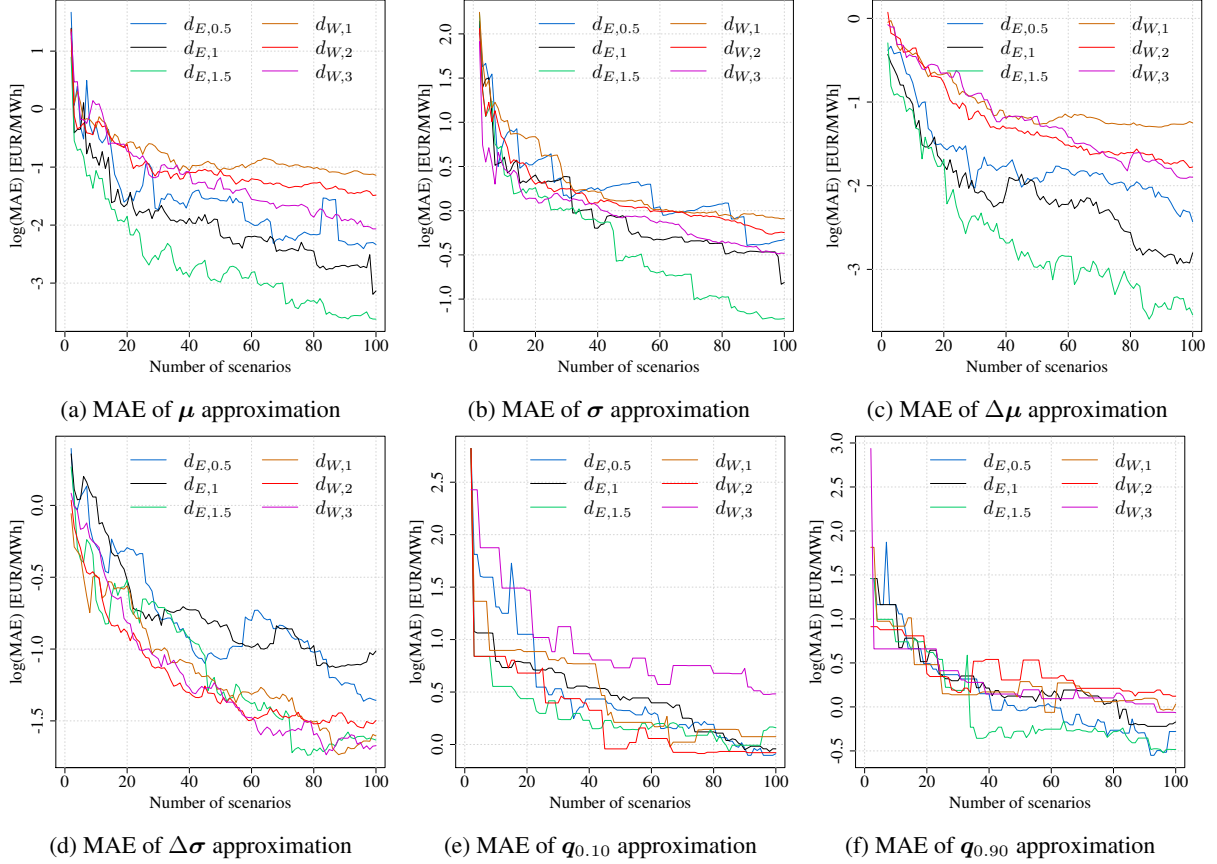


Figure 8: Scenario reduction results by energy and Wasserstein distances ( $d_{E,0.5}, d_{E,1}, d_{E,1.5}, d_{W,1}, d_{W,2}, d_{W,3}$ ). It shows the approximation accuracy in MAE (mean absolute error) of  $\mu$  (top left),  $\sigma$  (top center),  $\Delta\mu$  (top right),  $\Delta\sigma$  (bottom left), 10%-quantile  $q_{0.10}$  (bottom center) and 90%-quantile  $q_{0.90}$  (bottom right) for  $m = 2, \dots, 100$  scenarios of the  $n = 3653$  scenarios with monotonic smoothing spline fit.

the 10%- and 90%-quantile processes ( $q_{0.10} = (q_{0.10,1}, \dots, q_{0.10,24})$  and  $q_{0.90} = (q_{0.90,1}, \dots, q_{0.90,24})$ ). Figure 8 depicts the results of the scenario reduction for the six considered distances. In general, we observe that again the energy distance seems to be superior to the Wasserstein distance in the mean related measures (see 8a and 8c). For the energy distance  $d_{E,p}$ , the approximation results tend to get worse with decreasing  $p$ . For the Wasserstein distance  $d_{W,p}$ , the mean and variance characteristics also improve with increasing  $p$ . However, for the considered quantiles the picture is rather the other way around.

Additionally, we may deduce that the Wasserstein distance tends to replicate the tail and outlier properties better than energy distance. The latter is preferable for center properties which involve the full distribution, like mean and variance characteristics. This gets even clearer if we look at Figure 9. It shows the 100 selected paths out of the 3653 paths for all six metrics. We observe that reduced scenario sets of the Wasserstein distances  $d_{W,p}$  include more outlier trajectories than the energy distance reduction, and even more with increasing  $p$ . Consequently, the support of the full distribution is much better recovered. For  $d_{W,2}$  and  $d_{W,3}$ , even the overall minimum and maximum (see 1) is identified correctly. This comes at some cost of worse approximation in the non-tail and non-outlier properties. Thus, if scenario reduction is applied to stochastic optimization, the choice of the distance should likely depend on the stochastic properties that are crucial in the optimization. If mainly the tail and outlier events are relevant, then the Wasserstein distance is likely the first choice, otherwise the energy distance seems to be preferable.

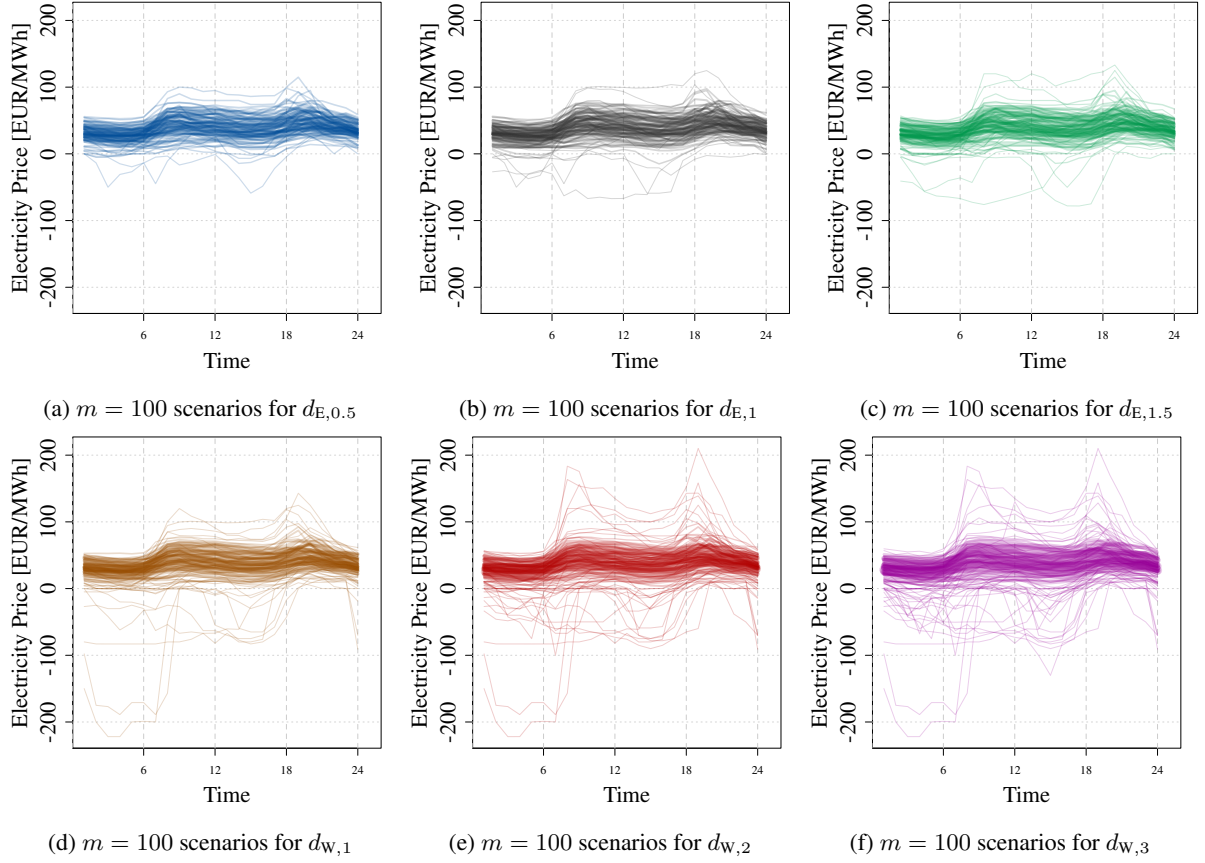


Figure 9: Illustration of randomly selected scenarios  $m = 100$  scenarios out of  $n = 3653$  by the energy distances  $d_{E,0.5}$ ,  $d_{E,1}$  and  $d_{E,1.5}$ , and Wasserstein distances  $d_{W,1}$ ,  $d_{W,2}$  and  $d_{W,3}$ .

## 5 Discussion and Conclusion

We illustrate that the energy distance is a suitable distance for ensemble and scenario reduction problems. It tends to provide better statistical/stochastic approximation properties than the popular Wasserstein distance which is vastly used in scenario reduction applications. Next to important characteristics like the approximation in the first two moments, this holds particularly for path-dependency properties. They are relevant in many applications, especially for those in stochastic programs in energy systems like storage, maintenance, and power trading optimization.

However, one drawback is that the reduction methods based on the energy distance is computationally slightly more demanding than the Wasserstein distance. This holds especially for the scenario reduction. Here, the Wasserstein distance has a simple explicit solution based on the redistribution rule which is linked to transportation problems. The energy distance on the other hand requires to solve a quadratic program with linear constraints. Due to the structure of the optimization problem Vavasis (1992) proves the existence of an algorithm that solves the quadratic program in quadratic time with respect to reduced scenario size. To our knowledge, such an algorithm is still unknown, further research should investigate potential optimization algorithms. Nevertheless, both the Wasserstein and energy distance lead to reduction problems that are NP-hard and require advanced search algorithms even for moderately sized problems. Sophisticated selection methods that work for the Wasserstein metrics can be applied to the energy distance as well, see e.g. Li and Gao (2019).

From the methodological point, the research can go in different directions. We only discussed briefly the impact of the parameter  $p$  in the energy distance  $d_{E,p}$  and Wasserstein distance  $d_{W,p}$ , and focused on the standard choices for  $p = 1$ . However, further investigations on the impact of  $p$  might be suitable. For heavy tailed data, the energy distance with  $p < 1$  should provide more stable results Székely and Rizzo (2013); Székely and Rizzo (2017).

Moreover, the energy distance can be generalized to a maximum mean discrepancy (MMD) concept using kernels (see e.g. Borgwardt et al. (2006); Székely and Rizzo (2017)). Then the distance measure is given by  $\mathbb{E}\kappa(\mathbf{X} - \mathbf{Y}) - \frac{1}{2}\mathbb{E}\kappa(\mathbf{X} - \mathbf{X}') - \frac{1}{2}\mathbb{E}\kappa(\mathbf{Y} - \mathbf{Y}')$  for suitable kernels  $\kappa$ . However, as noted by Sejdinovic et al. (2013) there is no superior kernel  $\kappa$  that serves well in all situations. Furthermore, popular kernels from machine learning like Gaussian or Laplacian kernels suffer disadvantages in high dimensions and do not satisfy scale equivariance, see Székely and Rizzo (2017). Thus, the standard energy distance (see (10)) seems to be an adequate natural candidate for scenario and ensemble reduction. Furthermore, the Sinkhorn divergence provides an interesting combination between the energy and Wasserstein distance, see e.g. Genevay et al. (2017). Here, further investigations with respect to scenario reduction problems might be useful to combine the beneficial properties from both worlds.

However, advantage of the low computational complexity of the Wasserstein distance for scenario reduction will be lost.

## References

- Andrychowicz, M., Olek, B., and Przybylski, J. (2017). Review of the methods for evaluation of renewable energy sources penetration and ramping used in the scenario outlook and adequacy forecast 2015. case study for poland. *Renewable and Sustainable Energy Reviews*, 74:703–714.
- Ball, K. (1992). Eigenvalues of euclidean distance matrices. *Journal of Approximation Theory*, 68(1):74–82.
- Bao, X., Sahinidis, N. V., and Tawarmalani, M. (2011). Semidefinite relaxations for quadratically constrained quadratic programming: A review and comparisons. *Mathematical programming*, 129(1):129.
- Biswas, P. P., Suganthan, P. N., Mallipeddi, R., and Amaratunga, G. A. (2019). Optimal reactive power dispatch with uncertainties in load demand and renewable energy sources adopting scenario-based approach. *Applied Soft Computing*, 75:616–632.
- Borgwardt, K. M., Gretton, A., Rasch, M. J., Kriegel, H.-P., Schölkopf, B., and Smola, A. J. (2006). Integrating structured biological data by kernel maximum mean discrepancy. *Bioinformatics*, 22(14):e49–e57.
- Chakraborty, S. and Zhang, X. (2019). Distance metrics for measuring joint dependence with application to causal inference. *Journal of the American Statistical Association*, 114(528):1638–1650.
- Di Somma, M., Graditi, G., Heydarian-Forushani, E., Shafie-Khah, M., and Siano, P. (2018). Stochastic optimal scheduling of distributed energy resources with renewables considering economic and environmental aspects. *Renewable energy*, 116:272–287.
- Dupačová, J., Gröwe-Kuska, N., and Römisches, W. (2003). Scenario reduction in stochastic programming. *Mathematical programming*, 95(3):493–511.
- Feng, Y. and Ryan, S. M. (2013). Scenario construction and reduction applied to stochastic power generation expansion planning. *Computers & Operations Research*, 40(1):9–23.
- Gazafroudi, A. S., Soares, J., Ghazvini, M. A. F., Pinto, T., Vale, Z., and Corchado, J. M. (2019). Stochastic interval-based optimal offering model for residential energy management systems by household owners. *International Journal of Electrical Power & Energy Systems*, 105:201–219.
- Genevay, A., Peyré, G., and Cuturi, M. (2017). Learning generative models with sinkhorn divergences. *arXiv preprint arXiv:1706.00292*.
- Glanzer, M. and Pflug, G. C. (2020). Multiscale stochastic optimization: modeling aspects and scenario generation. *Computational Optimization and Applications*, 75(1):1–34.
- Gneiting, T. and Katzfuss, M. (2014). Probabilistic forecasting. *Annual Review of Statistics and Its Application*, 1:125–151.
- Gneiting, T. and Raftery, A. E. (2007). Strictly proper scoring rules, prediction, and estimation. *Journal of the American Statistical Association*, 102(477):359–378.
- Gottschlich, C. and Schuhmacher, D. (2014). The shortlist method for fast computation of the earth mover’s distance and finding optimal solutions to transportation problems. *PloS one*, 9(10).
- Gröwe-Kuska, N., Heitsch, H., and Romisch, W. (2003). Scenario reduction and scenario tree construction for power management problems. In *2003 IEEE Bologna Power Tech Conference Proceedings*, volume 3, pages 7–pp. IEEE.
- Hayden, T. and Tarazaga, P. (1993). Distance matrices and regular figures. *Linear Algebra and its Applications*, 195:9–16.
- Heitsch, H. and Römisches, W. (2007). A note on scenario reduction for two-stage stochastic programs. *Operations Research Letters*, 35(6):731–738.
- Henrion, R., Küchler, C., and Römisches, W. (2009). Scenario reduction in stochastic programming with respect to discrepancy distances. *Computational Optimization and Applications*, 43(1):67–93.



- Keko, H. and Miranda, V. (2015). Impact of clustering-based scenario reduction on the perception of risk in unit commitment problem. In *2015 18th International Conference on Intelligent System Application to Power Systems (ISAP)*, pages 1–6. IEEE.
- Li, C.-L., Chang, W.-C., Cheng, Y., Yang, Y., and Póczos, B. (2017). Mmd gan: Towards deeper understanding of moment matching network. In *Advances in Neural Information Processing Systems*, pages 2203–2213.
- Li, Q. and Gao, D. W. (2019). Fast scenario reduction for power systems by deep learning. *arXiv preprint arXiv:1908.11486*.
- Muskulus, M. and Verduyn-Lunel, S. (2011). Wasserstein distances in the analysis of time series and dynamical systems. *Physica D: Nonlinear Phenomena*, 240(1):45–58.
- Nguyen, X. (2011). Wasserstein distances for discrete measures and convergence in nonparametric mixture models. Technical report, Citeseer.
- Park, S., Xu, Q., and Hobbs, B. F. (2019). Comparing scenario reduction methods for stochastic transmission planning. *IET Generation, Transmission & Distribution*, 13(7):1005–1013.
- Pflug, G. C. and Pichler, A. (2014). *Multistage stochastic optimization*. Springer.
- Rizzo, M. L. and Székely, G. J. (2016). Energy distance. *wiley interdisciplinary reviews: Computational statistics*, 8(1):27–38.
- Römisch, W. (2003). Stability of stochastic programming problems. *Handbooks in operations research and management science*, 10:483–554.
- Römisch, W. (2009). Scenario reduction techniques in stochastic programming. In *International Symposium on Stochastic Algorithms*, pages 1–14. Springer.
- Rujeerapaiboon, N., Schindler, K., Kuhn, D., and Wiesemann, W. (2018). Scenario reduction revisited: Fundamental limits and guarantees. *Mathematical Programming*, pages 1–36.
- Sejdinovic, D., Sriperumbudur, B., Gretton, A., and Fukumizu, K. (2013). Equivalence of distance-based and rkhs-based statistics in hypothesis testing. *The Annals of Statistics*, pages 2263–2291.
- Székely, G. J. and Rizzo, M. L. (2013). Energy statistics: A class of statistics based on distances. *Journal of statistical planning and inference*, 143(8):1249–1272.
- Szekely, G. J. and Rizzo, M. L. (2017). The energy of data. *Annual Review of Statistics and Its Application*, 4:447–479.
- Vavasis, S. A. (1992). Local minima for indefinite quadratic knapsack problems. *Mathematical Programming*, 54(1-3):127–153.
- Wang, J., Hazarika, S., Li, C., and Shen, H.-W. (2018). Visualization and visual analysis of ensemble data: A survey. *IEEE transactions on visualization and computer graphics*, 25(9):2853–2872.
- Zhou, Y., Shi, L., and Ni, Y. (2019). An improved scenario reduction technique and its application in dynamic economic dispatch incorporating wind power. In *2019 IEEE Innovative Smart Grid Technologies-Asia (ISGT Asia)*, pages 3168–3178. IEEE.
- Ziel, F. and Steinert, R. (2018). Probabilistic mid-and long-term electricity price forecasting. *Renewable and Sustainable Energy Reviews*, 94:251–266.